Reactions of Urea with Cu^+ in the Gas Phase: An Experimental and Theoretical Study

A. Luna, B. Amekraz, J. P. Morizur, and J. Tortajada*

Laboratoire de Chimie Organique Structurale, Université Pierre et Marie Curie, CNRS UMR 8587, Boite 45, 4 Place Jussieu, F-75252 Paris Cedex 05, France

O. Mó and M. Yáñez*

Departamento de Química, C-9, Universidad Autónoma de Madrid, Cantoblanco, 28049-Madrid, Spain

Received: October 5, 1999; In Final Form: January 4, 2000

The gas-phase reactions between Cu^+ and urea have been investigated by means of mass spectrometry techniques. The primary products formed in the ion source correspond to $[urea-Cu]^+$, $[(urea)_2-Cu]^+$, and $[Cu^+,C,N_2,H_2]$ complexes. The MIKE spectrum of $[urea-Cu]^+$ complex shows several spontaneous losses, namely, NH_3 and HNCO. A very weak peak corresponding to the loss of H_2O is also observed, as well as a minor fragmentation of the adduct ion to yield Cu^+. The structures and bonding characteristics of the different complexes involved in the urea−Cu^+ potential energy surface (PES) were investigated using density functional theory (DFT) at the B3LYP level of theory and a valence triple-ζ. Attachment of Cu^+ takes place preferentially at the carbonyl oxygen atom, while attachment at the amino group is 12.4 kcal/mol less exothermic. Insertion of the metal cation into the C−N bonds of the neutral is predicted to be slightly exothermic, in contrast with what was found for formamide and guanidine. The estimated urea−Cu^+ binding energy (62.3 kcal/mol) is 6.0 kcal/mol greater than that of formamide. The exploration of the PES indicates that there are several reaction paths leading to the loss of ammonia yielding as product ions $HNCOCu^+$ complexes where the metal cation is attached either to the oxygen or the nitrogen of the HNCO species. Also several reaction paths can be envisaged for the loss of HNCO, in which bisligated $[HNCO-Cu-NH_3]^+$ and $[OC(NH)-Cu-NH_3]^+$ complexes play an important role.

Introduction

Over the last 2 decades mass spectrometry has been proved to be a good experimental tool to investigate the gas-phase reactivity of many organic species. Lately, particular attention has been devoted to the study of the reactions between different neutral systems with metal monocations,[1] which normally lead to spontaneous fragmentations of the ion−molecule complexes initially formed. Our group has been interested in recent years in the study of these kind of reactions involving small molecules that can be used as model systems to understand the behavior of more complicated systems of biological relevance. In particular we have already studied the gas-phase reactions between Cu^+ and guanidine[2] and between Cu^+ and formamide,[3] and its isomers,[4,5] as suitable models of a peptide function. The aim of this paper is to carry out a similar study of the gas-phase reactions between urea and Cu^+. Urea and its derivatives are of industrial and biochemical relevance.[6] Urea itself is currently used to denature proteins in studies of protein folding and unfolding equilibria,[7] besides its capability in forming transition metal complexes.[8] Nevertheless, very little is known on its gas-phase reactivity and only very recently its gas-phase proton affinity[9] and its gas-phase acidity[10] were reported in the literature.

The paper is structured as follows: we shall present first the most important features of the chemical ionization-fast-atom bombardment (CI−FAB) mass spectrum associated with Cu^+ + urea reactions and the analysis of the MIKE spectrum of the $[urea-Cu]^+$ molecular ions. To complete the information on the $[urea-Cu]^+$ system, its collision-activated evolution was also studied by means of the CAD spectrum. To offer a rationale of the experimental findings, the urea−Cu^+ potential energy surface was explored through the use of density functional theory techniques.

Experimental Section

All experiments were carried out using a VG Analytical ZAB−HSQ hybrid mass spectrometer of BEqQ geometry, which has been described in detail previously.[11] Complexes were generated by the CI−FAB method.[12] The CI−FAB source was constructed from VG Analytical EI/CI and FAB ion source parts with the same modifications described by Freas et al.[12a] A copper foil of high purity has replaced the conventional FAB probe tip. "Naked" metal ions were generated by bombardment with fast xenon atoms (Xe gas 7−8 keV kinetic energy, 1−2 mA of emission current in the FAB gun). In these experimental conditions, $^{63}Cu^+$ and $^{65}Cu^+$ ions are then produced in a ratio which is close to that of their natural abundance (100/41 versus 100/45, respectively). The organic samples were introduced via a heated probe in a nonheated source. We have checked that under these experimental conditions urea does not decompose. We can assume that, due to the relatively high pressure in that source (10^{-2}−10^{-3} Pa), efficient collisional cooling of the generated ions takes place. Therefore, we will consider that excited states of the Cu^+ ions which could be formed in these experimental conditions are not likely to participate in the observed reactivity as already postulated by Schwarz et al.[12e] The ion beam of the Cu^+ adduct complexes, formed with urea, were mass selected (using an acceleration voltage of 8 kV) with

10.1021/jp9934634 CCC: $19.00
Published on Web 03/22/2000

the magnetic analyzer B. The ionic products of unimolecular fragmentations, occurring in the second field-free (2nd FFR) region following the magnet, were analyzed by means of mass-analyzed ion kinetic energy (MIKE)[13] by scanning the electric sector E. The CAD (collision activated dissociation) experiments were carried out in the same fashion, but we introduced Ar in the cell as the collision gas. The spectra were recorded at a resolving power (R) of ~1000.

Urea was purchased from Aldrich and used without further purification.

Computational Details

The theoretical treatment of the different systems included in this work was performed by using the B3LYP density functional approach in the Gaussian-94 series of programs.[14] This method has been found to be quite reliable as far as the description of metal cation−neutral complexes is concerned,[15] in particular when Cu^+ ions are involved.[2,3,16,17,18] The B3LYP approach is a hybrid method, which includes the Becke's three-parameter nonlocal exchange potential[19] with the nonlocal correlation functional of Lee, Yang, and Parr.[20] The geometries of the different species under consideration were optimized using the all electron basis of Wachters−Hay[21] for Cu ((14s9p5d1f)/[9s5p3d1f]) and the 6-311G(d,p) basis set for the remaining atoms of the system. The harmonic vibrational frequencies of the different stationary points of the potential energy surface (PES) have been calculated at the same level of theory used for their optimization in order to identify the local minima and the transition states (TS), as well as to estimate the corresponding zero-point energies (ZPE). To identify which minima are connected by a given TS, we have performed intrinsic reaction coordinate (IRC)[22] calculations at the same level of theory.

To obtain the final energies of the different species under study, we have used a 6-311+G(2df,2p) basis set for first-row atoms (H, C, O, and N) and a (14s9p5d/9s5p3d) Wachters−Hay's basis supplemented with a set of (1s2p1d) diffuse functions and with two sets of f and one set of g polarization functions for the Cu atom, so the following basis function and contraction (15s11p6d2f1g)/[10s7p4d2f1g] was used for Cu. It must be mentioned, however, that, for the sake of simplicity, we will maintain the nomenclature "6-311+G(2df,2p)" for all the atoms including Cu. As we have previously shown,[16] the binding energies for Cu^+ complexes obtained at the B3LYP/6-311+G(2df,2p)//B3LYP/6-311G(d,p) level are in reasonably good agreement with those estimated in the framework of the G2 theory.[23]

The bonding characteristics of the different species have been investigated by using two different techniques, namely, the atoms in molecules (AIM) theory of Bader[24] and the natural bond orbital (NBO) analysis of Weinhold et al.[25]

For this purpose in the first technique we have located the bond critical points, i.e., points where the electron density function $\rho(\mathbf{r})$ is at a minimum along the bond path and at a maximum in the other two directions. The Laplacian of the density $\Delta^2\rho(\mathbf{r})$, as it has been shown in the literature,[24] identifies regions of the space wherein the electronic charge is locally depleted ($\Delta^2\rho > 0$) or built up ($\Delta^2\rho < 0$). The former situation is typically associated with interactions between closed-shell systems (ionic bonds, hydrogen bonds, and van der Waals molecules), while the latter characterizes covalent bonds, where the electron density concentrates in the internuclear region. There are, however, significant exceptions to this general rule, mainly, when highly electronegative atoms are involved in the bonding, as in the F_2 molecule.[24] Hence, we have used instead the energy density[26] $H(\mathbf{r})$, which does not present these exceptions. In general, negative values of $H(\mathbf{r})$ are associated with a stabilizing charge concentration within the bonding region. The AIM analysis was performed using the AIMPAC series of programs.[27]

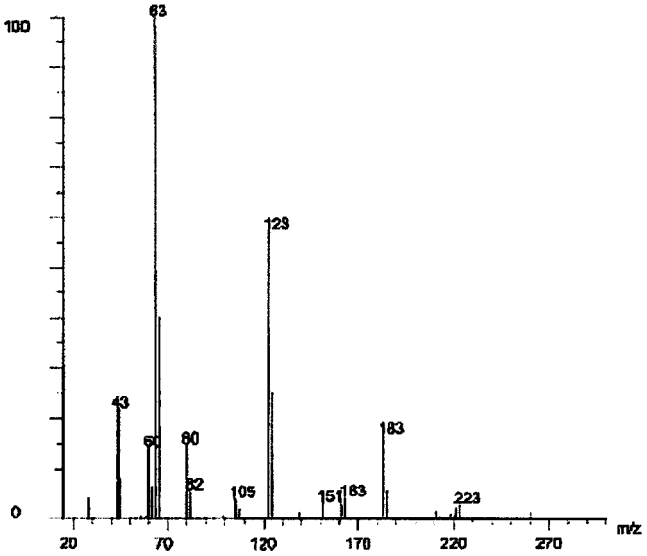

Figure 1. Mass spectrum that results from the reactions of Cu^+ sputtered from copper foil, with neutral urea.

Results and Discussion

Gas-Phase Reactivity. Figure 1 shows the mass spectrum that results from the gas-phase reactions of copper ions with urea. The existence of ^{63}Cu and ^{65}Cu isotopes leads to an easy identification of copper-containing ions. In ion−molecule reaction conditions, besides production of Cu^+, which is the base peak of the mass spectrum, several copper/organic product complexes were also observed. The Cu^+ ions react with neutral urea to produce mainly [urea−Cu^+] adduct ions at m/z 123, 125 (60%). This complex in turn reacts with another urea molecule to produce [$(urea)_2Cu^+$] at m/z 183, 185 (17%). The observed ions at m/z 105, 107 (5%) and m/z 80, 82 (15%) could correspond to [Cu^+,C,N_2,H_2] and to [Cu^+−NH_3] complexes, respectively. These ions could arise from the loss of water and HNCO of [urea−Cu^+] ions, respectively. All the peaks observed at m/z values under 63 correspond to fragmentation or protonation processes of urea, and therefore will not be discussed.

MIKES analysis was performed on [urea−Cu]$^+$ adduct ions to obtain information related to the structure, reactivity, and thermochemistry of these Cu^+/organic complex ions. The results presented here refer to the more abundant isotope ^{63}Cu-containing species.

Unimolecular Reactivity of [Urea−Cu]$^+$ Adduct Ions. The MIKE spectrum of the [urea−Cu]$^+$ complex presented in Figure 2 shows that the m/z 123 ion undergoes fragmentation by distinct pathways. The [urea−Cu]$^+$ complex ion gives rise to four spontaneous losses, the most important being that of NH_3 at m/z 106, which is the base peak of the MIKE spectrum, and that of HNCO at m/z 80 (35%). The minor fragmentation corresponds to the adduct ion dissociation to produce Cu^+ ion at m/z 63 (15%). The MIKE spectrum presents in addition a very weak peak at m/z 105 that corresponds to a loss of H_2O already observed in the ion source.

Under collision conditions one can note, in the resulting CAD spectrum displayed in Figure 3, that the intensity of the peak corresponding to the loss of H_2O increases showing that this

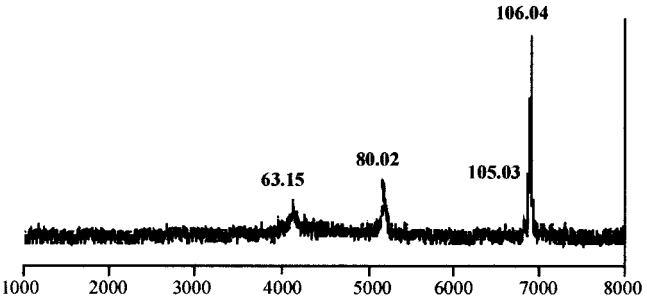

Figure 2. Metastable ion mass spectrum of urea−Cu^+ (*m*/*z* 123).

decomposing channel is a high energy demanding process compared with those leading to the loss of NH_3 and HNCO.

This spectrum also shows the presence of an ion at *m*/*z* 79, which can correspond either to NH_2Cu^+ or to CuO^+. In the former case this would be an indication that Cu^+ cation can be attached to the less basic center of urea. In the latter case the accompanying product would be a quite stable diaminocarbene. As we shall show later the cleavage of the C−N bond in nitrogen attached urea−Cu^+ complexes is more favorable than the cleavage of the C═O bond in oxygen-attached urea−Cu^+ complexes, so very likely this peak corresponds to NH_2Cu^+. In this respect it is worth noting that a similar peak was recently reported by Wu and Wesdemiotis[28] in the CAD spectra of Cu-$(NH_3)_n^+$ ($n = 1$ or 2) complexes. The peak corresponding to Cu^+ increases when the pressure of the collision gas increases, but never becomes the dominant product.

The ability of Cu^+ to be dicoordinated is well documented[2,3,29,30] and corroborated, in our case, by the presence in the CI−FAB mass spectrum (Figure 1) of the [$(urea)_2$−Cu^+] adduct ions at *m*/*z* 183. In this respect, the competitive losses of neutral NH_3 and HNCO might be explained as proceeding via the Cu^+-bound heterodimer [HNCO−Cu^+−NH_3] as a common intermediate which undergoes competitive dissociations leading to the two fragment ions at *m*/*z* 80 and *m*/*z* 106. However, as we shall discuss later, the complex [HNCO−Cu^+−NH_3] loses only HNCO, the loss of ammonia being associated with different local minima of the PES.

To analyze these experimental findings, we have investigated alternative mechanisms in forthcoming sections, through a detailed study of the [urea−Cu] potential energy surface by means of DFT calculations.

Characteristics of the [Urea−Cu^+] Complexes. To provide a rationale of the most outstanding features of the MIKE and CAD spectra associated with urea−Cu^+ interactions in the gas phase, we have explored the corresponding PES through the use of DFT calculations. The optimized geometries of the different stationary points located on this PES are shown in Figure 4, and their total and relative energies are summarized in Table 1. Figure 4 and Table 1 also include the possible products of the Cu^+−urea reactions.

It can be observed that the attachment of the metal monocation to the carbonyl oxygen atom of the neutral is 12.9 kcal/mol more favorable than the attachment to the nitrogen of the amino group. Interestingly, this energy gap is only slightly smaller than that reported in the literature[9] for the corresponding oxygen- and nitrogen-protonated species. It is also important to note that the insertion of Cu^+ into the C−NH_2 bond is estimated to be exothermic. This implies a significant difference with respect to the reactivity of other similar bases such as guanidine[2] and formamide,[3] for which this insertion process was estimated to be always endothermic.

It is also worth noting that the estimated urea−Cu^+ binding energy (62.3 kcal/mol) is 6 kcal/mol higher than that estimated for formamide−Cu^+ complexes,[3] showing the enhancement of the intrinsic basicity of the carbonyl group due to the presence of a second amino group in the system. The gap between the Cu^+ binding energies of urea and formamide is only slightly smaller than that found between their proton affinities.[9,31] The activation of the C═O linkage is larger in urea than in formamide,[3] and the O−Cu linkage stronger and shorter, consistently with its larger binding energy. In fact, as shown in Table 2, on going from neutral urea to complex **1**, the charge density at the C═O bond critical point decreases significantly while the energy density becomes less negative. A concomitant reinforcement of the C−N bonds takes place, this effect being greater for the bond, which is trans to the metal cation. Also, coherently, the charge density at the O−Cu bond critical point is larger and the energy density more negative in urea−Cu^+ complexes than in formamide−Cu^+ ones.[3] These charge redistributions are also mirrored in a shift of the stretching frequencies. Upon Cu^+ attachment to the carbonyl oxygen atom, the C═O stretching frequency appears shifted 118 cm^{-1} to the red, while the C−N stretching frequencies are blue-shifted by 115 cm^{-1}.

Attachment of the metal monocation at the amino nitrogen also leads to significant charge redistribution. As shown in Table 2, the C−N bond directly affected by the substitution is significantly activated, while the other is reinforced. Accordingly, the first C−N linkage lengthens significantly and its stretching frequency becomes 164 cm^{-1} smaller. The C═O linkage also reinforces slightly and its stretching frequency appears 38 cm^{-1} blue shifted.

To rationalize the gas-phase reactivity of urea−Cu^+, we have envisaged three different mechanisms depending on the nature of the first step. The first two correspond to the attachment of the Cu^+ to one of the two basic sites of the neutral, which would

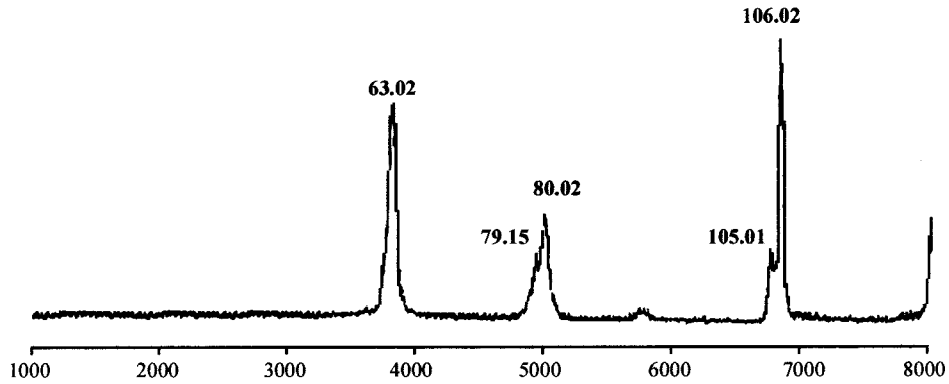

Figure 3. CAD spectrum of urea−Cu^+ (*m*/*z* 123).

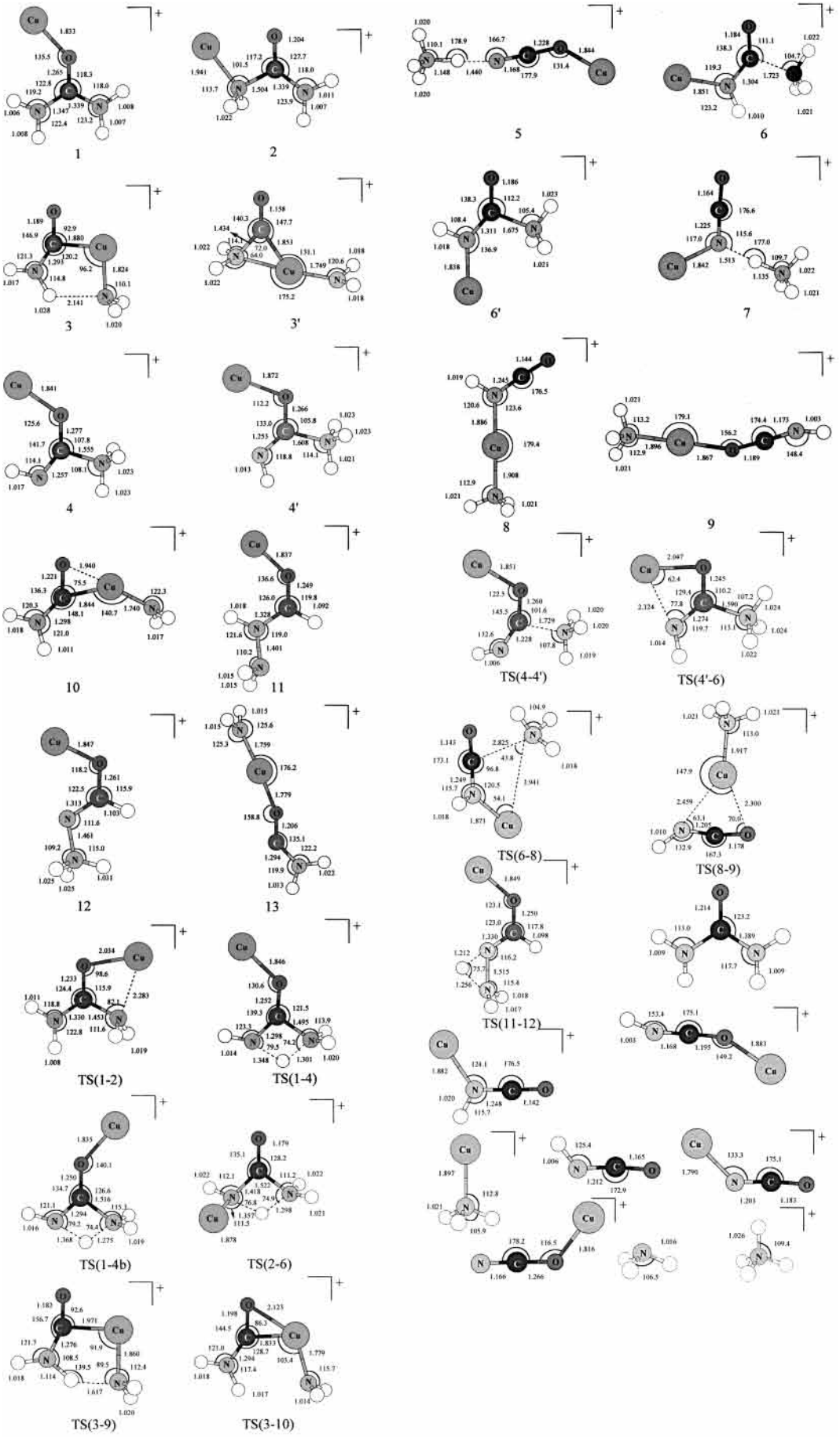

Figure 4. B3LYP/6−611G(d,p) optimized geometries of the stationary points of the urea−Cu^+ potential energy surface and of the possible products of the urea−Cu^+ reaction. Bond lengths are in angstroms and bond angles in degrees.

TABLE 1: B3LYP/6-311+G(2df,2p) Total Energies (*E*) and B3LYP/6-311G(d,p) ZPE (in hartrees) for the Different Species under Consideration: Relative Energies ΔE (in kcal/mol), Include the Corresponding ZPE Correction.

	E	ZPE	ΔE
1	−1865.639 332	0.064 567	0.0(0.0a)
2	−1865.619 790	0.065 530	12.9(8.4[a])
3	−1865.541 547	0.061 757	59.6
3′	−1865.530 694	0.062 2 00	66.7
4	−1865.589 078	0.065 660	32.2
4′	−1865.586 655	0.064 6 36	33.1(32.1[a])
5	−1865.609 928	0.060 994	16.2
6	−1865.603 375	0.064 483	22.5
6′	−1865.595 676	0.065 138	27.8
7	−1865.619 265	0.061 785	10.8
8	−1865.667 623	0.063 820	−18.2
9	−1865.658 865	0.061 852	−14.0
10	−1865.556 375	0.063 149	51.2
11	−1865.568 720	0.065 237	44.7
12	−1865.551 034	0.065 707	56.1
13	−1865.523 633	0.061 011	70.4
TS(1−2)	−1865.624 319	0.064 642	9.5(10.2[a])
TS(1−4)	−1865.551 914	0.060 667	52.4
TS(1−4b)	−1865.547 570	0.060 438	55.0
TS(2−6)	−1865.538 649	0.060 451	60.6
TS(3−9)	−1865.541 980	0.059 019	57.6
TS(3−10)	−1865.539 207	0.061 42	60.7
TS(4−4′)	−1865.566 962	0.061 760	43.7
TS(4′-6)	−1865.588 641	0.064 176	31.6(33.7[a])
TS(6−8)	−1865.590 668	0.060 545	28.0
TS(8−9)	−1865.624 945	0.061 5 08	7.1
TS(11−12)	−1865.478 595	0.058 6 55	97.2
$Cu(HN)CO^+$	−1808.990 224	0.024 159	
$HNCOCu^+$	−1808.981 639	0.021 994	
urea	−225.362 573	0.063 768	
Cu^+	−1640.176 694	0.000 000	
NH_3	−56.586 387	0.034 299	
HNCO	−168.749 174	0.021 343	
$Cu-NH_3+$	−1696.857 206	0.038 918	
NH_4^+	−56.923 116	0.049 486	
NCOCu	−1808.615 822	0.011 967	
CuNCO	−1808.656 4 340	0.012 569	

[a] The values between parentheses correspond to B3LYP/6-311G(d,p) + ZPE level.

TABLE 2: Charge Densities (ρ) and Energy Densities ($H(\mathbf{r})$) Evaluated at the Corresponding Bond Critical Points: All Values in au

		CO	CN[a]	CN[b]	Cu−X
urea	ρ	0.416	0.309	0.309	
	$H(\mathbf{r})$	−0.706	−0.387	−0.387	
1	ρ	0.366	0.334	0.341	0.111
	$H(\mathbf{r})$	−0.583	−0.456	−0.471	−0.017
2	ρ	0.425	0.247	0.337	0.101
	$H(\mathbf{r})$	−0.729	−0.240	−0.468	−0.026

[a] Indicates the CN closest to the Cu atom. [b] Indicates the CN farthest to the Cu atom.

be, in principle, the most likely ones. However, because, as we have mentioned above, the insertion into the C−N bond lies below the reactants in energy, we have considered it of interest to explore this third possibility, also. In what follows we have not considered the possible mechanisms associated with the loss of water because, as we have mentioned in preceding sections, this corresponds to a very weak peak in the MIKE spectrum whose intensity increases under CAD conditions, showing that this decomposing channel is a high energy demanding process.

Oxygen-Attachment Mechanism. The energy profile associated with the unimolecular reactivity of species **1** has been plotted in Figure 5. This figure shows that species **1** evolves to yield species **4** through an appropriate 1,3-H shift. Quite interestingly, there are two alternative processes, which involve different activation barriers. When the hydrogen atom is transferred from the amino group which is cis with respect to the metal toward the amino group which is trans, the estimated activation barrier is 2.6 kcal/mol lower than the alternative process in which the hydrogen is transferred from the latter toward the former. Both processes lead however to the local minimum, **4**, i.e., the hydrogen shift through the **TS(1−4b)** transient species is accompanied by a simultaneous displacement of Cu so that a sole local minimum, with the metal trans with respect to the ammonia molecule, can be located.

It can be observed that the $C-NH_3$ distance in species **4** is surprisingly small (See Figure 4). An investigation of its bonding characteristics, by means of the NBO method, shows the existence of a quite strong C−N dative bond involving the lone pair of the ammonia molecule. Consistently, the charge density at the corresponding bond critical point is large (0.211 au) and the energy density negative (−0.203 au) showing that this interaction has a large covalent character. Also unexpectedly, the products of the $C-NH_3$ bond cleavage, $HNCOCu^+ + NH_3$, lie only 7 kcal/mol above species **4**, which seems to be in contradiction with the strength of the $C-NH_3$ bond. This may be explained if one takes into account that the $C-NH_3$ bond fission leads to a reinforcement of the HN−C bond. Actually, a NBO analysis shows that, while this linkage has a double-bond character in species **4**, it has a nearly triple-bond character in the isolated $HNCOCu^+$ molecular ion, and the bond shortens from 1.257 to 1.168 Å (See Figure 4).

A migration of the NH_3 molecule toward the NH group yields species **5**. This process implies a barrier of ca. 11 kcal/mol, which was estimated by scanning the $C-NH_3$ distance. It is important to mention that this migration led to species **5** and never to species **9** (see Figure 4), in which the ammonia molecule is attached to the metal, even though **9** is estimated to be 30.2 kcal/mol more stable than **5**. We have tried many other alternative ways to connect species **4** and **9**, as an internal rotation around the C−O bond, or a migration of the NH_3 molecule toward the copper atom, but all of them failed.

Structure **4** presents a conformer **4′**, which lies 0.9 kcal/mol higher in energy. Both species are connected through the **TS(4−4′)** transient species, which corresponds to a flipping of the −NH group, and which lies 11.4 kcal/mol above species **4**. Conformer **4′** can also dissociate to yield $HNCOCu^+ + NH_3$ or evolve to structure **5**. It can also yield structure **6**, where the metal cation is attached to the imino nitrogen, through a very low (1.4 kcal/mol, at the B3LYP/6-311G(d,p) level) activation barrier. This is a very important point since, as we shall show later when discussing nitrogen attached species, structure **6** plays a crucial role in the loss of HNCO.

It is also worth noting that a spontaneous proton-transfer accompanies the formation of species 5. Indeed, as shown in Figure 4, species **5** is not a $CuOCNH^+\cdots NH_3$ hydrogen bonded complex, but a $CuOCN\cdots H_4N^+$ one. This is a somewhat unexpected result since the estimated proton affinity of the CuOCN neutral species to yield the $CuOCNH^+$ structure (223.0 kcal/mol, see Table 1) is almost 20 kcal/mol higher than the proton affinity of ammonia. Actually, as illustrated in Figure 5, the $CuOCNH^+ + NH_3$ dissociation limit lies 20.4 kcal/mol below the $CuOCN + NH_4^+$ one. Nevertheless, a NBO analysis shows that the neutral CuOCN species has a noticeable zwiterionic character reflected in a very large dipole moment (8.5 D), with a large positive charge (+0.738) located at the Cu atom and an almost equally large negative charge (−0.524) located at the nitrogen. As a consequence, even though the non

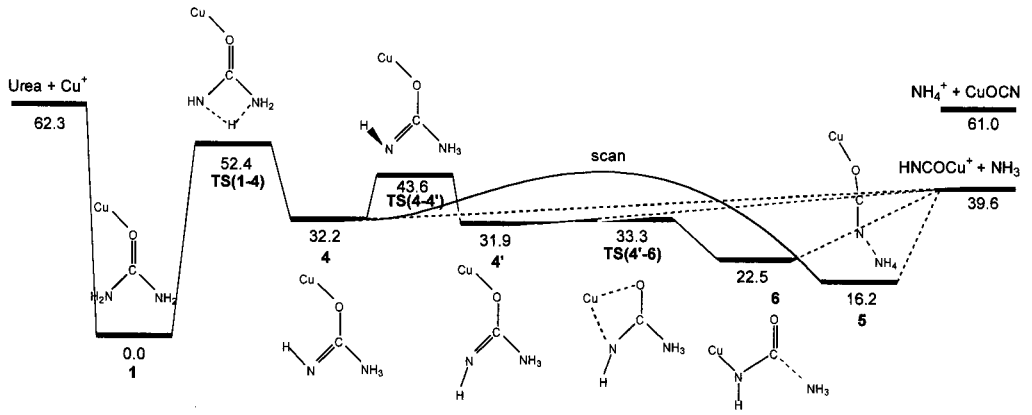

Figure 5. Energy profile corresponding to the unimolecular decomposition of the oxygen- attached urea−Cu^+ complex **1**. Relative energies in kcal/mol.

interacting NH_4^+ + CuOCN species lie 20.4 kcal/mol higher in energy than the NH_3 + $CuOCNH^+$ ones, the interaction between the former is much stronger so that, when both subunits are at short distances, the $CuOCN\cdots H_4N^+$ arrangement lies lower in energy than the $CuOCNH^+\cdots NH_3$ one.

Although the most favorable process should correspond to the dissociation of **4**, the formation of some amount of species **5** cannot be completely discarded. Therefore, it would be necessary to assess which would be the most likely dissociation products of this species. What is obvious is that its dissociation into the two interacting subunits (NH_4^+ + CuOCN) should occur without activation barrier, while its dissociation into $CuOCNH^+$ + NH_3 should be preceded by a proton transfer process which very likely involves an activation barrier. To investigate this point a survey of the proton-transfer mechanism within structure **5** was carried out for two different N···N distances. The first selected N···N value was that of the equilibrium conformation of complex **5**, the other one corresponded to an increase of this distance by 0.3 Å. For an N···N distance equal to that in the equilibrium conformation of species **5**, in agreement with the conclusions of Gónzalez et al.,[32] a single-well proton-transfer potential energy curve was found. However, when the N···N distance was enlarged by 0.3 Å a double-well potential energy curve was found, in which the $CuOCNH^+\cdots NH_3$ minimum is almost degenerate with the $CuOCN\cdots NH_4^+$ one. The important point is that the proton-transfer barrier (7.1 kcal/mol) is rather small as compared with the energy gap between the NH_4^+ + CuOCN and $CuOCNH^+$ + NH_3 dissociation limits.[34] Therefore, we can conclude that, even if species **5** is formed, it would never dissociate to CuOCN + NH_4^+. The absence of NH_4^+ is simply due to thermochemistry. This is in agreement with the fact that NH_4^+ was never observed in the MIKE spectrum.

It can be observed that all the barriers in Figure 5 lie below the reactants in energy and therefore the aforementioned mechanisms would be favored with respect to the loss of Cu^+, although this possibility cannot be completely discarded.

We have also explored the possibility of a 1,2H shift from one of the amino groups of species **1** toward the carbon atom. This hydrogen shift implies a simultaneous migration of the other amino group so that the local minimum **11** is attained. However, this structure lies quite high in energy and it cannot be a precursor for the loss of ammonia because the transition state connecting structures **11** and **12** (See Figure 4), **TS(11−12)**, lies above the entrance channel.

Another alternative mechanism would correspond to an amino migration toward the metal cation followed by a proton-transfer who would connect species **1** and **9**. However, this possible route can be discarded, because the local minimum, **13**, resulting from the first step of this mechanism lies about 70 kcal/mol above species **1.** More importantly, since Cu favors linear arrangements, the subsequent proton-transfer process would be not feasible.

Nitrogen-Attachment Mechanism. The energy profile associated with the unimolecular reactivity of species **2** has been plotted in Figure 6. As we have mentioned above, the attachment of Cu^+ to the amino group of urea is 12.9 kcal/mol less exothermic than the attachment to the carbonyl oxygen, but the binding energy is still sizably large (49.4 kcal/mol). However, it must be taken into account that the practically barrier free evolution from the nitrogen-attached species **2** to the oxygen-attached structure **1** (through the **TS(1−2)** transient species) is similar to what was found before for guanidine−Cu^+ complexes.[2] A 1,3-H shift through the **TS(2−6)** transition state would connect species **2** and **6**. Obviously, this route cannot compete with the evolution to yield **1**, but we must recall here that species **6** can be also formed from structure **4′**, and therefore, studying its further evolution is important for the rationalization of urea−Cu^+ experimental reactivity. Structure **6** would eventually dissociate into NH_3 and $CuNHCO^+$, since, as shown in Figure 4, it can be viewed as a tightly bound ion dipole complex between these two moieties. This loss of ammonia yields a different cation than that obtained upon dissociation of structures **4** and **4′**. In the first case the metal is attached to the nitrogen atom of the HNC═O species, while in the second it is attached to the oxygen atom. Species **6** can alternatively evolve through an ammonia transfer to yield a more stable structure **7**. We could not locate the transition state corresponding to this process and the energy barrier was estimated by scanning the C−NH_3 distance. It should be noted that a proton-transfer process, similar to the one described above for species **5** accompanies this ammonia migration. More importantly, the estimated energy barrier for this process is quite large (ca. 22 kcal/mol) and therefore the evolution from **6** to **7** cannot compete with the direct dissociation of **6** into $Cu(NH)CO^+$ + NH_3, and therefore species **7** should not be formed in a significant amount. This is consistent with the fact that, due to the thermochemistry, NH_4^+ is not experimentally observed as reaction product.

As mentioned above, structure **6** plays an important role in urea−Cu^+ reactions because it may evolve through the transition state **TS(6−8)** to yield species **8**, which is the global minimum of the $[Cu, H_4, C, N_2, O]^+$ PES, and a suitable precursor for the loss of HNCO. The large stability of species **8** reflects the ability of Cu^+ to yield dicoordinated structures, also found to be particularly stable in (glycine−Cu^+),[30] (guanidine−Cu^+)[2] and (formamide−Cu^+)[3] interactions. More importantly, these kinds

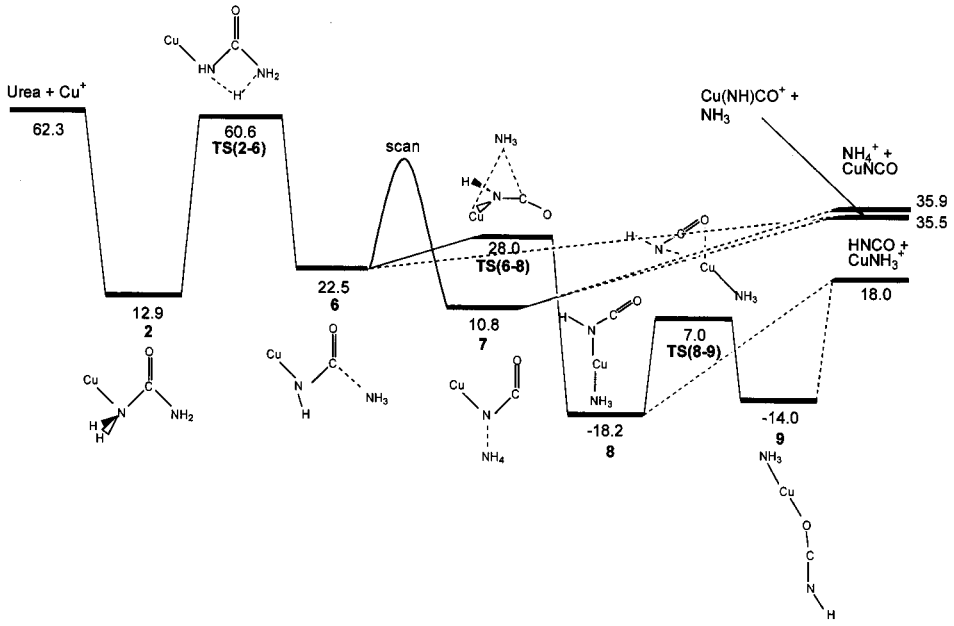

Figure 6. Energy profile corresponding to the unimolecular decomposition of the nitrogen- attached urea−Cu^+ complex **2**. Relative energies in kcal/mol are referred to species **1**.

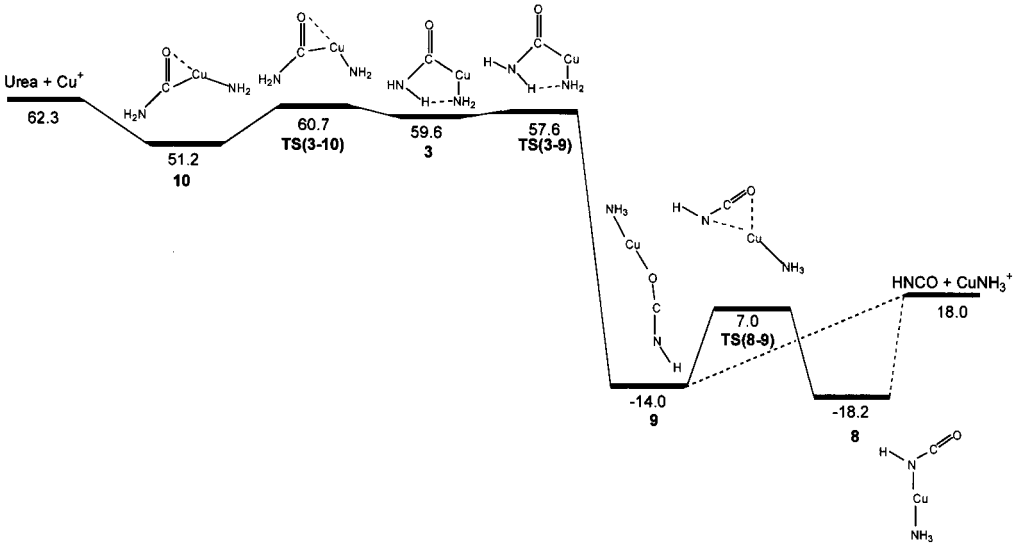

Figure 7. Energy profile corresponding to the unimolecular decomposition of the urea−Cu^+ complex **3**, corresponding to the insertion of the metal cation into the C−N bond of the neutral. Relative energies in kcal/mol are referred to species **1**.

of dicoordinated species play an important role in the reactivity of these systems, since they are the necessary precursors for the formation of $CuNH_3^+$ ions, which, as we mentioned in previous sections, are experimentally observed products of the urea−Cu^+ reactions. Indeed our theoretical calculations indicate that the Cu^+ binding energy of ammonia is 17.5 kcal/mol higher than that of HNCO when Cu^+ attaches at the nitrogen atom. Hence, as far as complex **8** is concerned, the dissociation into $CuNH_3^+$ + HNCO prevails over the dissociation into NH_3 + $CuHNCO^+$. It must be observed however, that a migration of the Cu−NH_3 moiety would connect species **8** and **9** through a relatively low activation barrier (**TS(8−9)**). In any case, structure **9** would also dissociate preferentially into $CuNH_3^+$ + HNCO, because the Cu^+ binding energy at the oxygen atom of HNCO is also smaller (by 21.6 kcal/mol) than that of ammonia.

In summary, we must conclude that in urea−Cu^+ reactions the fragmentation of these dicoordinated complexes leads exclusively to the loss of HNCO, while the loss of ammonia is the result of the fragmentation of molecular complexes, such as **4**, **4′,** or **6**, where the NH_3 moiety is not attached to the metal.

According to our results, structure **6** must be a minor species because, although the barrier for the **4′** → **6** isomerization is rather small (See Figure 5), the energy barrier associated with the **4** → **4′** tautomerization process is higher, and higher than the energy required to dissociate **4** into $HNCOCu^+$ + NH_3. Since **6** is the precursor of both, **8** and **9**, these must be also minor species. This is in agreement with the experimental evidence, which shows that the loss of HNCO is a minor process. On the other hand, the formation of species from the nitrogen-attached adduct **2** cannot compete with the **2** → **1** isomerization process.

We have also explored an alternative route to evolve from species **2** to **8**, through an amino migration toward the metal cation followed by a proton transfer. However, this rearrangement produces only two local minima, namely, **3**, which lies very high in energy, and **3′** which lies above the entrance

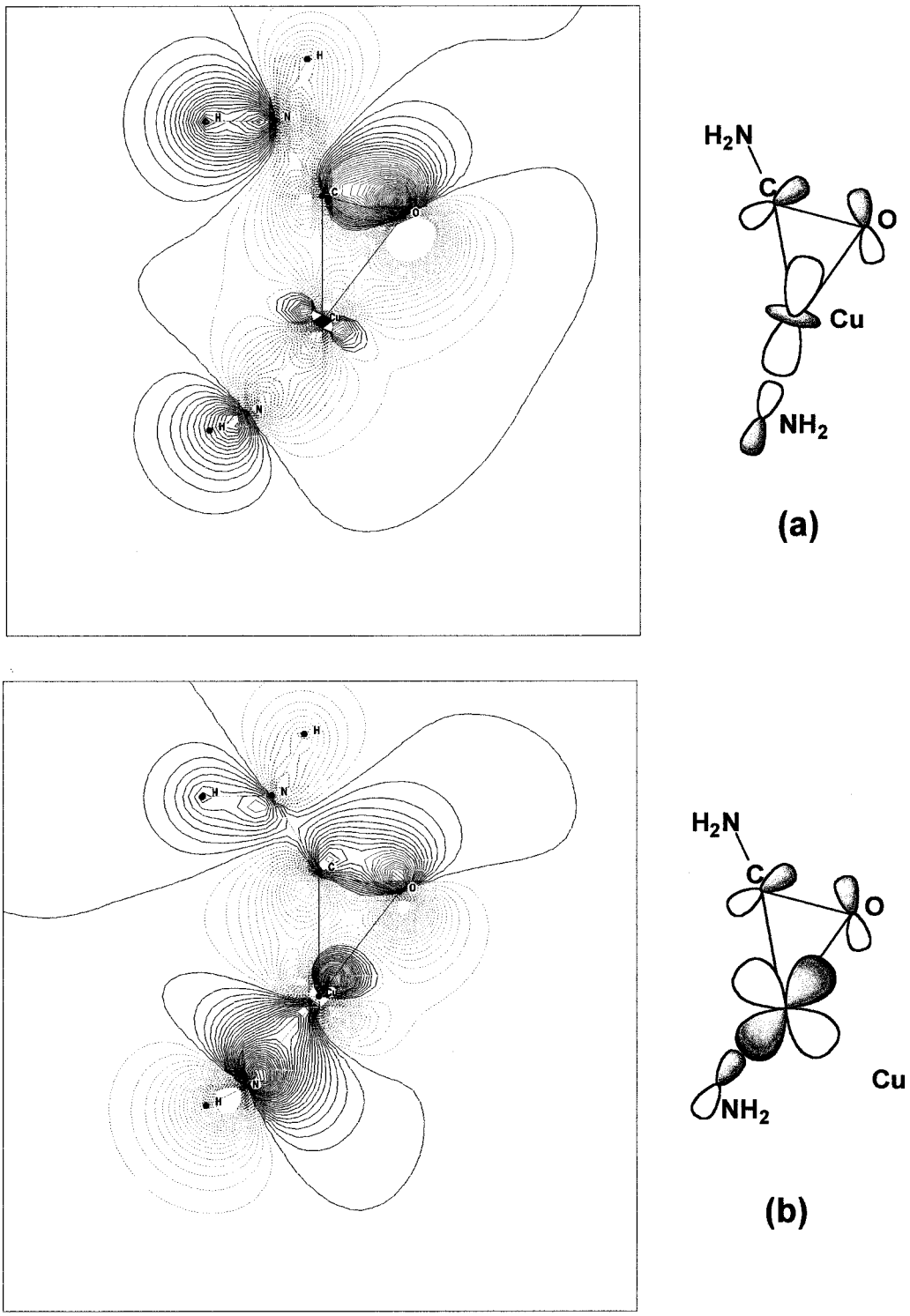

Figure 8. Contour maps of the molecular orbitals associated with the bonding of Cu to the C═O bond and the amino group in complex **10**.

channel. In this respect it is also important to mention that an $O{=}C{-}NH_2{-}Cu{-}NH_2$ arrangement is not stable as it collapses to structure **3′**. These two local minima can be viewed as structures in which the metal cation inserts into the $C{-}NH_2$ bond, and they will be discussed in detail in the next section.

Insertion Mechanism. In this section we shall discuss the possible reactions pathways associated with the unimolecular reactivity of species **3,** which is the result of the insertion of Cu^+ into the C−N bond of the neutral (See Figure 7). It seems obvious that, in contrast with attachment processes, insertion of the metal cation into the C−N bond cannot be a direct process. We have tried, with no success, to locate the transition structure that would connect the entrance channel urea + Cu^+ with species **3**. However, we have found that when the metal cation approaches the C−N linkage a C−O−Cu three-membered ring is formed, apparently without activation barrier, yielding species **10**. In this structure the Cu^+ is apparently tricoordinated rather than dicoordinated as in complexes **8** or **9**; however, no bond critical point could be found between Cu and O, i.e., the metal cation is only bonded to the carbon and the nitrogen atoms. An inspection of the canonical molecular orbitals shows that actually Cu interacts simultaneously with the π-type orbitals of the carbonyl group and with the p orbitals of nitrogen atom. These interactions involve the d_{z^2} and the d_{xy}

orbitals of Cu, respectively. As illustrated in Figure 8, one of these MO's has a bonding interaction with the C−O orbital and with a p orbital of the nitrogen, while the other one is bonding with respect to the carbon and antibonding with respect to the oxygen.

Structure **10** can evolve to yield the local minimum **3** by closing the C−Cu−N angle in order to favor the formation of an intramolecular hydrogen bond between both amino groups, which has been characterized by a topological analysis of its charge density. Although an H−N···N intramolecular hydrogen bond is formed, the system slightly destabilizes, because the departure from linearity of the C−Cu−N fragment implies a weakening of the two linkages in which Cu participates (See Figure 4). Once species **3** is formed, a 1,4-H transfer through the **TS(3−9)** transient species yields structure **9**, which can dissociate into $CuNH_3^+$ + HNCO or alternatively evolve to yield the global minimum **8**, which eventually would dissociate into the same products.

Conclusions

The primary products formed in the reactions between urea and Cu^+ in the gas phase, in CI−FAB conditions, correspond to $[urea-Cu]^+$, $[(urea)_2-Cu]^+$, and $[Cu^+, C, N_2, H_2]$ complexes. The MIKE spectrum of $[urea-Cu]^+$ complex shows several spontaneous losses, namely, NH_3 and HNCO. A very weak peak corresponding to the loss of H_2O is also observed, as well as a minor fragmentation of the adduct ion to yield Cu^+.

Our B3LYP/6-311+G(2df,2p)//B3LYP/6-311G(d) calculations show that the attachment of Cu^+ takes place preferentially at the carbonyl oxygen atom, while attachment at the amino group is 12.4 kcal/mol less exothermic. This energy gap is only slightly smaller than that reported in the literature for the corresponding oxygen- and nitrogen-protonated species[9] Quite interestingly our theoretical estimates predict the insertion of the metal cation into the C−N bonds of the neutrals to be exothermic, while similar processes for formamide[3] and guanidine[2] were predicted to be endothermic at the same level of theory.

The estimated urea−Cu^+ binding energy (62.3 kcal/mol) is 6.0 kcal/mol greater than that of formamide.[3] This enhancement of the gas-phase basicity, due to the resonance stabilizing effect of the second amino group, and to the increase of the polarizability of the molecule, is only slightly smaller than that found between the proton affinities of these two species.[9,31] This seems to confirm[33] that the behavior of Cu^+ as a reference acid resembles closely that of the proton.

The exploration of the PES indicates that several reaction paths leading to the loss of ammonia can be envisaged. In the (HNCO)−Cu^+ product ions the metal cation is attached either to the oxygen or the nitrogen of the HNCO species, depending on the characteristics of the precursor. The most important point is that in these processes ammonia is never attached to the metal cation. In fact, the linkage Cu^+-NH_3 is so strong, that all the species which present this moiety finally lose HNCO, but never ammonia. Our exploration of the PES shows that the precursors for the loss of HNCO are systematically diccordinated species similar to the ones postulated before[2,3] to explain the unimolecular reactivity of guanidine−Cu^+ and formamide−Cu^+ complexes. Similar bisligated complexes were also proposed by Freiser et al.[29] to explain the reactivity of acids, esters, and ketones with Cu^+. Also, Wesdemiotis et al.[30] evidenced the formation of triligated complexes in the case of glycine−Cu^+ complexes by means of neutralization−reionization techniques.

The fact that the most favorable process in urea + Cu^+ reactions is the loss of ammonia, while the loss of HNCO corresponds to a minor fragmentation, is also in agreement with the characteristics of the theoretically estimated PES. Actually, the most favorable reaction path, with origin in the oxygen attached species, leads to the loss of ammonia. In contrast, the loss of HNCO is a secondary unimolecular decomposition of the oxygen-attached complex or the result of the insertion of the metal cation into the C−N bond, which in both cases would occur via multistep mechanisms.

Acknowledgment. This work has been partially supported by the DGES Project PB96-0067 and by a NATO Cooperative Grant CRG.973140. We thank Dr. M. Alcamí for helpful suggestions. Generous allocations of computational time at the Centro de Computacion Cientifica de la Facultad de Ciencias (CCCFC) de la UAM and at the I.D.R.I.S. (Orsay) are also acknowledged.

References and Notes

(1) Freiser, B. S., Ed. *Organometallic Ion Chemistry*; Kluwer Academic Publishers: Dordrecht, 1995.

(2) Luna, A.; Amekraz, B.; Morizur, J.-P.; Tortajada, J.; Mó, O.; Yáñez, M. *J. Phys. Chem.* **1997**, *101*, 5931.

(3) Luna, A.; Amekraz, B.; Tortajada, J.; Morizur, J.-P.; Alcamí, M.; Mó, O.; Yáñez, M. *J. Am. Chem. Soc.* **1998**, *120*, 5411.

(4) Luna, A.; Morizur, J.-P.; Tortajada, J.; Alcamí, M.; Mó, O.; Yáñez, M. *J. Phys. Chem.* **1998**, *102*, 4652.

(5) Alcamí, M.; Mó, O.; Yáñez, M.; Luna, A.; Morizur, J.-P.; Tortajada, J. *J. Phys. Chem.* **1998**, *102*, 10120.

(6) *Chem. Eng. News* **1987**, *65*, 21. March, J. *Advanced Organic Chemistry*, 4th ed.; John Wiley & Sons: New York, 1992. Franco, L.; Andrei, M.; Andrea, C. *Science* **1994**, *266*, 801. Lam, P. Y. S.; Jadhav, P. K.; Eyermann, C. J.; Hodge, C. N.; Ru, Y.; Bacheler, L. T.; Meek, J. L.; Otto, M. J.; Rayner, M. M.; Wong, Y. N.; Chang, C.; Weber, P. C.; JAckson, D. A.; Sharpe, T. R.; Erikson-Viitanen, S. *Science* **1994**, *263*, 380. Thomas, G. C.; George, S. *Chem. Rev.* **1997**, *97*, 829.

(7) Neri, D, Billeter, M.; Wider, G.; Wuthrich, K. *Science* **1992**, *227*, 1559. Liepinsh, E.; Otting, G. *J. Am. Chem. Soc.* **1994**, *116*, 9670. Schellman, J. A.; Gassuer, N. C. *Biophys. Chem.* **1996**, *59*, 259.

(8) Theophanides, T.; Harvey, P. D. *Coord. Chem. Rev.* **1987**, *76*, 237.

(9) Wang, F.; Ma, S.; Zhang, D.; Cooks, R. G. *J. Phys. Chem. A* **1998**, *102*, 2988.

(10) Ma, S.; Wang, F.; Cooks, R. G. *J. Mass Spectrom.* **1998**, *33*, 943.

(11) Harrison, A. G.; Mercer, R. S.; Riener, E. J.: Young, A. B.; Boyd, R. K.; March, R. E.; Porter, C. J. *Int. J. Mass Spectrom. Ion Processes* **1986**, *74*, 13.

(12) (a) Freas, R. B.; Ross, M. M.; Campana, J. E. *J. Am. Chem. Soc.* **1985**, *107*, 6195. (b) Freas, R. B.; Campana, J. E. *J. Am. Chem. Soc.* **1985**, *107*, 6202. (c)Mestdagh, H.; Morin, N.; Rolando, C. *Tetrahedron Lett.* **1986**, *27*, 33. (d) Drewello, T.; Eckart, K.; Lebrilla, C. B.; Schwarz, H. *Int. J. Mass Spectrom. Ion Processes* **1987**, *76*, 13. (e) Hornung, G.; Schröder, D.; Schwarz, H. *J. Am. Chem. Soc.* **1995**, *117*, 8192. (f) Chamot-Rooke, J.; Tortajada, J.; Morizur, J.-P. *Eur. Mass Spectrom.* **1995**, *1*, 471.

(13) (a) Cooks, R. G.; Beynon, J. H.; Caprioli, R. M.; Lester, G. R. *Metastable Ions*; Elsevier: New York, 1973. (b) Cooks, R. G., Ed. *Collision Spectroscopy*; Plenum Press: New York, 1978.

(14) Frisch, M. J.; Trucks, G. W.; Schlegel, H. B.; Gill, P: M.W.; Johnson, B. J.; Robb, M. A.; Cheeseman, J. R.; Keith, T. A.; Peterson, G. A.; Montgomery, J. A.; Raghavachari, K.; Al-Laham, M. A.; Zakrzewski, V. G.; Ortiz, J. V.; Foresman, J. B.; Cioslowski, J.; Stefanow, B. B.; Nanayaklara, A.; Challacombe, M.; Peng, C. Y.; Ayala, P. Y.; Chen, W.; Wong, M. W.; Andres, J. L.; Replogle, E. S.; Gomperts, R.; Martin, R. L.; Fox, D. J.; Binkley, J. S.; Defrees, D. J.; Baker, J.; Stewart, J. P.; Head-Gordon, M.; Gonzalez, C.; Pople, J. A.; *Gaussian 94*; Gaussian, Inc.: Pittsburgh, PA, 1995.

(15) (a) Llamas-Saiz, A. L.; Foces-Foces, C.; Mó, O.; Yáñez, M.; Elguero, E.; Elguero, J. *J. Comput. Chem.* **1995**, *16*, 263. (b) Florián, J.; Johnson, B. G. *J. Phys. Chem.* **1994**, *98*, 3681. (c) Bauschlicher, C. W. *Chem. Phys. Lett.* **1995**, *246*, 40. (d) Martell, J. M.; Goddard, J. D.; Erikson, L. A. *J. Phys. Chem.* **1997**, *101*, 1927. (e) Cui, Q.; Musaev, D. G.; Svensson, M.; Sieber, S.; Morokuma, K. *J. Am. Chem. Soc.* **1995**, *117*, 12366. (f) Ricca, A.; Bauschlicher, C. W. *J. Phys. Chem.* **1995**, *99*, 9003. (g) Ziegler, T. *Chem. Rev.* **1991**, *91*, 651.

(16) Luna, A.; Amekraz, B.; Tortajada, J. *Chem. Phys. Lett.* **1997**, *266*, 31.

(17) Hoyau, S.; Ohanessian, G. *Chem. Phys. Lett.* **1997**, *280*, 266.

(18) Kemper, P. R.; Weis, P., Bowers, M. T.; Maitre, P. *J. Am. Chem. Soc.* **1998**, *120*, 13494

(19) (a) Becke, A. D. *J. Chem. Phys.* **1993**, *98*, 5648. (b) Becke, A. D. *J. Chem. Phys.* **1992**, *96*, 2155.

(20) Lee, C.; Yang, W.; Parr, R. G. *Phys Rev.* **1988**, *B37*, 785.
(21) (a) Wachters, A. J. H. *J. Chem. Phys.* **1970**, *52*, 1033. (b) Hay, P. J. *J. Chem. Phys.* **1977**, *66*, 4377.
(22) González, C.; Schlegel, H. B. *J. Chem. Phys.* **1989**, *90*, 2154.
(23) Curtiss, L. A.; Raghavachari, K.; Trucks, G. W.; Pople, J. A. *J. Chem. Phys.* **1991**, *94*, 7221.
(24) Bader, R. F. W. *Atoms in Molecules. A Quantum Theory;* Oxford University Press: Oxford, 1990.
(25) Weinhold, F.; Carpenter, J. E. *The Structure of Small Molecules and Ions*; Plenum Press: New York, 1988.
(26) (a) Cremer, D.; Kraka, E. *Croat. Chim. Acta* **1984**, *57*, 1529. (b) Cremer, D.; Kraka, E. *Angew. Chem., Int. Ed. Engl.* **1984**, *23*, 627.
(27) The AIMPAC programs package has been provided by J. Cheeseman and R. F. W. Bader.
(28) Wu, J.; Wesdemiotis, C. *Chem. Phys. Lett.* **1999**, *303*, 243.
(29) Burnier, R. C.; Byrd, G. D.; Freiser, B. S. *Anal. Chem.* **1980**, *52*, 1641.
(30) Polce, M. J.; Beranova, S.; Nold, M. J.; Wesdemiotis, C. *J. Mass Spectrom.* **1996**, *31*, 1073.
(31) Lias S. G.; Bartmess, J. E.; Liebman, J. F.; Holmes, J. L.; Levine, R. D.; Mallard, W. J. *J. Phys. Chem. Ref. Data* **1988**, *17*, Suppl. 1.
(32) González, L.; Mó, O.; Yáñez, M. *J. Phys. Chem.* **1998**, *102*, 1356.
(33) Although to quantitatively estimate the proton-transfer barrier a more flexible basis set (including diffuse functions) would be needed, the possible changes in the value of the barrier would not affect our conclusions, since as mentioned above, the difference between the proton-transfer barrier (7 kcal/mol) and the energy gap between both exit channels (21 kcal/mol) is very large.
(34) Jones, R. W.; Staley, R. H. *J. Am. Chem. Soc.* **1982**, *104*, 2296.